A Review of 15 Years Full-Scale Seismic Testing at the HDR

L. MALCHER
Kernforschungszentrum Karlsruhe, Karlsruhe, FRG
H. STEINHILBER
Fraunhofer Institut für Betriebsfestigkeit, Darmstadt, FRG

1 GENERAL OVERVIEW

The HDR Safety Program is carried out by the Karlsruhe Nuclear Research Center (KfK) on behalf of the German Federal Ministry for Research and Technology (BMFT). The Program has been subdivided into several Sub Projects according to the main activities in the field of Reactor Safety Research and actual questions of licensing procedure and public interest. This presentation deals with the earthquake investigations, exclusively.

The general objective of the project is the experimental verification of calculation tools and procedures. To get an objective picture about the capability of design calculation methods, the activities within the whole program are usually carried out as a joint effort by various parties: while KfK is responsible for the performance of the experiments, data acquisition, comparisons and evaluations, the calculations are performed by specialized institutions. Here, the project management tries to maintain a reasonable balance between industrial participants, independent institutions and authorities responsible for the licensing of nuclear power plants. Besides the independence of the results obtained, this procedure has another advantage: the findings and conclusions of the evaluation process are directly transferred to the engineering community.

2 HDR TEST FACILITY

The experiments are carried out in a former 100 MW nuclear power plant, the so-called Superheated Steam Reactor (HDR), Fig. 1. The plant is located in Kahl, 40 km east of Frankfurt/Main. It was an experimental and prototypical facility built from 1965 through 1969. The reactor was shut down in 1971 after only some 2000 hours of operation because of difficulties with the superheated fuel elements and the simultaneous economic success of boiling and pressurized water reactors. After extensive decommissioning and conversion measures, the plant is fully available since 1975 for safety related technical experiments.

The HDR reactor building, Fig. 2, is a reinforced concrete and steel structure approximately 52 m high. It is embedded to a

SMiRT 11 Transactions Vol. K (August 1991) Tokyo, Japan, © 1991

depth of 13 m giving an overall height of the building of 65 m. The outer diameter is 22.4 m. The internal concrete structure consists of 2 concentrical cylinders interconnected by numerous walls and floors separating compartments for the mechanical equipment. In the center, the reactor pressure vessel is located with a height of 10 m, an inner diameter of 3.0 m and a wall thickness of 14.2 cm.

A steel containment with a wall thickness of approximately 3 cm encloses the inner structure, separated from it by a 2 cm thick styrofoam layer. The steel cylinder extends to a height of 40 m, where a polar crane is located (10 m above the operating floor) and is topped with the hemispherical steel dome. Personal and equipment hatches are connected to the steel containment shell. The third part of the building, the external containment out of reinforced concrete, is also a cylindrical shell with a hemispherical dome. The wall thickness is 60 cm and the reinforcement is poor, because the HDR was not designed against horizontal loads other than wind loads.

The fourth part is the basement with the foundation slab and a massive inner cylinder supporting the inner structure like an egg in an egg-cup. Structurally, this can be regarded as the only connection between inner steel containment and concrete containment. The two shells are independent of each other at all other points. The annulus between concrete and steel shell is 60 cm wide and accessible.

On the left side of the reactor building the crane and equipment tower, on the right side the office and auxiliary building are to be seen.

Because the site, Fig. 3, was previously used for brown coal mining activities, a specific means for improving the soil characteristics by vibration injection of gravel columns down to the solid clay layers in 20 m depth had been taken before construction. The ground water table is to be found at - 6 m.

By means of an electrically heated boiler of 4 MW, as well boiling water as pressurized water conditions can be achieved in the mechanical equipment. Besides that, extensive facilities for measurement and data acquisition were installed. 400 fast (5 kHz) and 200 slow (2.5 Hz) measuring channels can be sampled at the same time. This measurement data acquisition system is connected through a data link with a data base at the Project HDR in the Karlsruhe Nuclear Research Center.

Besides the experimental data, this data base contains the results of calculations, which are performed for all experiments. Thus a sound basis is formed for unique data evaluation and verification of codes, mathematical modeling practices and assumptions of parameters and boundary conditions.

3 EARTHQUAKE INVESTIGATIONS

In the time frame between 1975 and 1988 a series of test campaigns have been performed, Fig. 4:

- Low Level and Modal Vibration Tests (1975 and 1982)
- Moderate Level Tests (1979)
- Hot Snapback Tests (1983)

- Seismic Margins Tests of the Reactor Building (1986)
- Seismic Margins Tests of a Piping System (1988)
- Pipe Failure Tests (1988)

Mechanical and electrodynamic shakers, explosives, snapback devices, impact hammers and servohydraulic actuators were used for excitation of the structures, which are also listed in Fig. 4. About 25 institutions have been participating with analytical efforts in parallel to the experiments. Results have been presented during all SMIRT-Conferences since 1977.

While Fig. 5 gives an overview about the range of shaker forces vs. excitation frequencies, some of the shakers are shown in Fig. 6 and 7. In Fig. 7 also the functional principle of the 10 MN peak force coast down shaker (ANCO, MK 16) is to be seen: (1.) the two balanced shaker arms at an individual starting frequency, (2.) the begin of the folding process and (3.) the moment of coupling together both arms forming now the eccentricity of the system.

4 EXTRACT OF RESULTS

Within this brief summarizing report only a rough overview can be given about the test performance and results obtained during the whole program. The chosen examples refer to the reactor building, the pressure vessel, a tank and piping systems.

4.1 Reactor Building

During the Low Level Tests in 1975, the HDR reactor building was excited by buried explosives and eccentric mass shakers. The biggest shaker available at that time, ANCO's MK 14 with an eccentric mass of 147 kgm, had one rotating arm and provided an omnidirectional horizontal excitation in the frequency range to approximately 3 Hz (Fig. 6). The shaker tests consisted of sweeps for natural frequency identification and steady state test runs at and around natural frequencies. The latter tests served to evaluate the mode shapes by varying the locations of the limited number of accelerometers. The buildings fundamental modes of vibration were 2 rocking modes at 1.52 and 1.57 Hz and 2 structural modes at 2.63 and 2.81 Hz. In the structural modes, the internal concrete structure with the steel liner was moving out of phase to the external concrete containment. These modes were characterized as first bending modes of the building, though a considerable part of the deflection results from the flexibility of the basement, where both structures are coupled.

Six different institutions were charged to establish 10 different building models including a variety of possible soil idealizations (soil springs derived from half space theory, semi-finite elements, FE-models), Fig. 8. The simplest beam model had 42 degrees of freedom (DOF), the most complicated nearly 10,000. The latter was then used to compare the qualities of the so called "static condensation method", a mathematical method to reduce the complexity of a FE-model, with the common engineering practice of reduction by judgement, i.e. through an

appropriate idealization. The 9,500 DOF were reduced in two steps to 66 DOF, a number comparable to that of the simplest model.

All of these modeling attempts were made "blind", i.e. without any knowledge of test results, on the basis of the original drawings of the HDR building and using the results of a seismic evaluation of dynamic soil properties. The calculated natural frequencies are compared in Fig. 9 with those from the tests. Obviously, most models predicted the rocking modes at lower frequencies than observed. For the beam models, the under prediction was around 30 to 40 percent, independent of the way how the soil was idealized. The large variance of the calculated rocking frequencies for the more complex models demonstrated that the use of advanced tools is no guarantee for good results. The model with the finest degree of discretization showed mode shapes which were nearly not comparable to the measured ones.

Regarding the lowest structural modes, the bending vibration, the beam models generally overpredicted these frequencies, because the rigid coupling of internal and external structures in the models did not correspond to reality. The real flexibility of the reactor building's basement can be reproduced better by a shell model.

A series of **Moderate Level Tests** took place in 1979, using considerably improved measurement and data analysis techniques. Also tests with vessels and piping at design temperature and pressure were performed. The applied shaker forces were raised by a factor of approximately 12 compared to the low level tests, Fig. 5.

The individual shaker test runs were performed as computer controlled incremental step tests in different frequency ranges. At each step, the vibrators were hold at a constant frequency long enough for all transient effects to decay so that only the steady- state response of the structure was recorded by the computerized data acquisition system. Signals from 98 accelerometers on the building and on pipes and vessels were recorded simultaneously for several cycles and immediately reduced to amplitude and phase information. After each test run, these data were normalized by the shaker forces and analyzed with respect to natural frequencies, damping values and mode shapes.

The calculations and theoretical investigations accompanying this test series concentrated on specific topics such as soil-structure interaction, load dependency of damping or the applicability of simplified computation methods.

For the **Seismic Margins Tests (SHAG)** of the HDR Reactor Building in 1986, a very large shaker was designed and constructed by ANCO with the assistance of LBF, where numerous functional and design calculations where performed. This shaker is, to our knowledge, the most powerful eccentric mass shaker in the world. The basic principle is, that the two shaker arms are in a balanced position while the speed is increased up to a preset final frequency depending on the attached weights. Immediately after decoupling from the drive system, an explosive bolt is fired, releasing the movable arm, which swings around and couples with the other arm, forming now a large eccentric mass, Fig. 7. While coasting-down through the buildings resonances, the shaker transfers its energy to the building. Masses between 4 and 25

tons on each of the two shaker arms were applied. Starting frequencies varied between 8 and 1.6 Hz for eccentricities from 4700 kgm and 67 000 kgm. The maximum force exceeded 10 000 kN.

The SHAG test series was planned such as to provide the ultimate loading of the HDR reactor building without global failure. Local damage was accepted. The test objectives could be reached without utilising the highest possible shaker eccentricity. Extensive safety calculations before the tests and measurements allowed to exceed the calculated ultimate load limits for some building components by factors of up to 10 compared to a normal design type calculation, or up to a factor of 3, compared to a best estimate calculation, Fig. 10. But margins of this order of magnitude may only be expected for complex structural parts like the basement region, whose numerous walls and floors are simplified for calculations. In addition those structures behave "fail-safe" in some sense, since ,after failure of one member, the loads are transmitted through others. Simple structures like the cylindrical shell of the external concrete containment have smaller margins. The latter component limited the applicable loads during the SHAG tests at a level slightly above the calculated (best estimate) value, Fig. 10.

During the tests with the greatest eccentricities, the rocking mode frequencies dropped significantly, indicating the decrease of the soil shear stiffness, Fig. 11. In parallel, the rocking mode damping was increased due to the hysteretic soil damping, which adds on to the response-independent radiation damping, Fig. 12. Large concentric cracks and subsidence of the soil were observed around the building, as well as a foundation settlement of 3 to 11 mm and a permanent deflection of 20 mm of the top of the dome. Impact occurred between the containment and the crane tower. The connecting bridge to the office building was slightly displaced.

The excitation levels achieved are comparable to intensities 7 to 8 on the modified Mercalli Scale, which is in the range of the strongest possible earthquakes in Germany, though the reactor building was not designed against seismic events.

4.2 Reactor Pressure Vessel

The dynamic behavior of the pressure vessel (RPV) was investigated during the Moderate Level Test Series in 1979 and 1983, using shakers and snapback devices. The "blind" calculations with FE-Models generally underpredicted the first bending frequency of the RPV, since the corrugated tube compensator, which seals the annulus around the RPV against the flooding water, had an unexpected stiffening effect. As can be seen in Fig. 13, this component is also responsible for the very different vibration behavior of the RPV in cold and hot conditions, respectively. With increasing temperature, the gap between structural elements firmly attached to the RPV and those fixed to the building was closed due to the radial thermal expansion. This adds to the radial stiffness of the compensator and, since the cylindrical parts are not ideally round, increases the damping by friction. Thus, damping values of 40% were evaluated from the snapback tests at 285°C, i.e. after one to two cycles the vibrations had decayed.

4.3 Flood Water Storage Tank

In contrast to the RPV, the flood water storage tank in the auxiliary building is a thin walled shell structure. For the shaker and snapback tests in 1979 and 1982 it was partly filled with water. The most important result of these tests was the incredibly low damping of the fundamental bending mode. Fig. 14 serves to illustrate that free vibrations after a snapback test showed nearly no decay and could be measured for minutes. The vibration amplitudes of about 3 to 4 m/s^2 with a peak of 16 m/s^2 at the beginning correspond to strains of 5 o/oo (well above yield) at the lower head, where the tank is supported by a welded box-shaped pedestal on four short beams.

4.4 Piping Systems

A number of piping systems of the HDR were investigated during the program, Fig. 4. These were as well rather simple pipes (SRL, PDL) as complex, branched systems including pipes of different diameters, manifolds, valves and other components (URL, VKL). Natural frequencies and mode shapes of FE-models established on the basis of drawings showed in general major differences to the measured ones, especially for the complex systems and for the measurements at low levels of excitation. The differences can be attributed to differences between nominal and real pipe dimensions and to nonlinearities in supports (gaps, friction). These types of nonlinearities dominate the response for small vibrations, while they are less important for large amplitudes. Low level tests are therefore of limited value for piping investigations.

The VKL-piping system was object of all three high level test campaigns. It consists of a number of pipe runs ranging in nominal size from 100 to 300 mm with the main two loops connected to the HDU vessel and the DF 16 manifold, Fig. 15. Different dynamic support systems were designed by various participants in the VKL-tests (NRC, EPRI, CEGB, KWU). These systems ranged from the very stiff (US-typical) NRC configuration with rigid struts and snubbers to the very flexible HDR configuration with essentially only dead weight supports, Fig. 16. Also included were alternative support systems using energy absorbers or seismic stops as snubber replacement devices.

The top of DF 16 is about 3 m below the operating floor, where the coast-down shaker was mounted during the SHAG tests. Three shaker runs with different eccentricities and starting frequencies of 8, 5.6 and 4 Hz provided an indirect excitation of the VKL in excess of the defined HDR-SSE spectrum, Fig. 17. During the Seismic Margins Tests and the Pipe Failure Tests, both in 1988, the VKL was directly excited by means of two servohydraulic cylinders acting simultaneously in the same horizontal direction at the DF 16 and hanger location H5, Fig. 15. An artificially generated earthquake time history with a duration of 15 sec. and a zero perod acceleration of 6 m/s^2 was used. Fig 17 shows the input spectra from tests with 6 different support configurations. All configurations were tested at and above design level, i.e. between 100% and 300% SSE. Two configu-

rations, namely the flexible KWU system and the stiff NRC system, were tested up to 800% SSE.

At the most highly stressed locations of the piping system strain ranges of 1.5% and accumulated residual strains of 1.2% were measured. The level D allowable stresses for the pipe material correspond to strain ranges of approximately 0.44% (linear correspondence). This strain value was exceeded at one location about 100 times and up to a factor of three, Fig. 18. In actual, the resistance of the material against cyclic loading is much higher, because the allowable stresses for seismic design correspond to values which would lead to plastic collapse under static loading. The application of these limit values to the small number of short duration load peaks occurring during earthquakes is very conservative.

The dependency of damping values on the load level was investigated for the earthquake tests, by means of parameter-variation calculation. The modal damping values for these calculations were individually fitted by comparing measured and calculated spectral response values. The results are compared in Fig. 19 with damping values prescribed in or recommended for regulatory guides. Obviously no definite correlation exists between modal stress and modal damping. It is equally clear that by using damping values of 4% (new KTA) or 5% (PVRC), the calculation of the piping stresses from dynamic loadings, which is one of the steps in the design procedure, may not necessarily provide conservative results.

For the final pipe failure tests (ERI) a pre-damaged straight pipe section and elbow out of highly ductile ferrite 15 MnNi 6 3 were welded into the most highly stressed area A and B respectively, Fig. 15. The circumferential oriented crack in the straight pipe extended over 60° and had a crack depth to wall thickness ratio of a/t=0.4. In the elbow, a crack field had developed during cyclic tests over the whole length along the bend flanks with maximum depths of a/t=0.17. The ERI tests were performed under pressurized water conditions (240°C, 70 bar). The time history of nominal stresses at location A is illustrated in Fig. 20 in a very condensed form. It included 58 earthquake tests at 100, 400 and 600% SSE and 50 sine burst tests for accelerated crack propagation until leakage occurred. As shown in Fig. 21, the initial crack angle of 60° had not increased.

The pre-cracked elbow did not fail even under a second test series of again 108 tests with loadings up to 800% SSE. Fatigue failures at other locations ended these tests. Failure of piping systems out of ductile material under earthquake loading seem to be highly unlikely.

5 ACKNOWLEDGEMENT

Many colleagues from the United States, the United Kingdom, Switzerland, and from numerous institutions in Germany contributed substantially so the success of the HDR earthquake investigations in the past 15 years. The authors wish to thank all of them for their help through expertise, advices, participation and assistance.

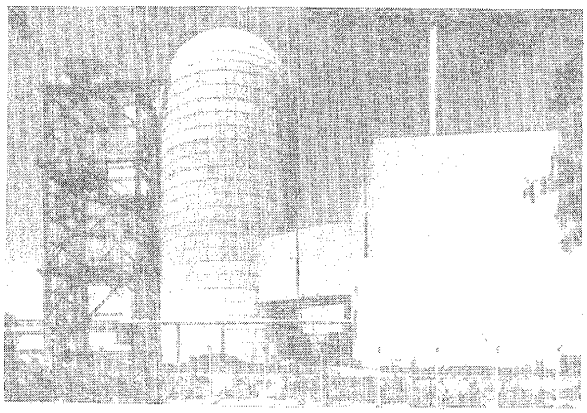

Fig.1: HDR Test Facility

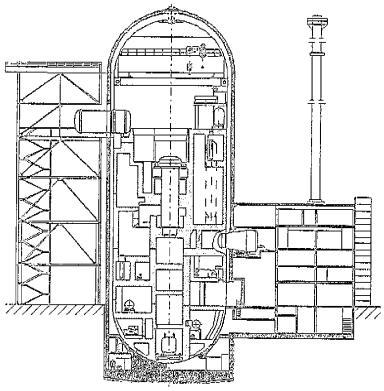

Fig.2: Cross Section of the HDR Test Facility

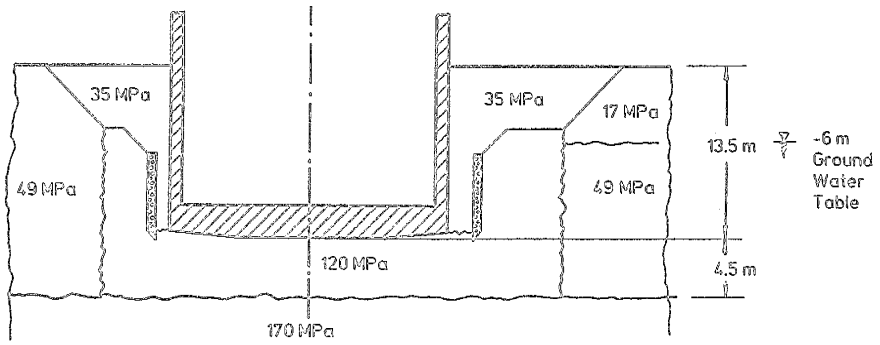

Fig.3: Shear Moduli of the HDR Site

TEST SERIES (Year)	EXCITATION	STRUCTURE	PEAK RESPONSE Acc. (Strain)	SMiRT-PAPERS
Low Level Tests (1975)	Ecc. Mass Shaker 40 kN Explosives 10 kg Snapback 25 kN	Reactor Building Steam Generator Recirculation Pipe URL Saturated Steam Pipe SRL	0.6 m/s² 0.7 m/s² 0.5 m/s² (0.05 ‰)	SMiRT 4 (1977) K8/5, K8/6 SMiRT 5 (1979) K13/2, K13/3
Modal Vibration Tests (1982)	Servohydr. Shaker 13.3 kN El.-Dyn. Shaker 0.45 kN	Steel Containment Flood Water Storage Tank		SMiRT 7 (1983) K15/4, K15/5
Moderate Level Tests (1979)	Ecc. Mass Shaker 500 kN Explosives 5 kg Snapback 220 kN Rockets 400 kN	Reactor Building Reactor Pressure Vessel Flood Water Storage Tank Recirculation Pipe URL Primary Steam Pipe PDL	0.8 m/s² 4 m/s² 16 m/s² (5‰) 16 m/s² (0.55‰) 51 m/s² (0.5‰)	SMiRT 6 (1981) K14/1 to 5 SMiRT 7 (1983) K2/8 to 12, K4/7, K9/7, K9/8, K12/12
Hot Snapback Tests (1983)	Snapback 400 kN	Reactor Pressure Vessel Primary Steam Pipe PDL	25 m/s² 171 m/s² (1.2‰)	SMiRT 8 (1985) K19/7
Seismic Margin Tests Building (1986)	Ecc. Mass 10,000 kN Coasi-Down Shaker	Reactor Building Test Pipe Loop VKL	4 m/s² (50 mm) 75 m/s² (0.4‰)	SMiRT 8 (1985) K21/4, K21/5 SMiRT 9 (1987) K9/1, K9/2, K9/3, K14/5, K14/7, Sess.JK1 SMiRT 10 (1989) K32/1
Seismic Margin Tests Piping (1988)	Servohydraulic Actuators 600 kN	Test Pipe Loop VKL	395 m/s² (9.12‰)	SMiRT 10 (1989) K 28/1, K28/2 SMiRT 11 (1991) K32/2, K32/3
Pipe Failure Tests (1988)	Servohydraulic Actuators 800 kN	Test Pipe Loop VKL with Predamaged Segments	300 m/s² (6.5‰)	SMiRT 10 (1989) G 13(F)/1

Fig.4: Earthquake Test Program

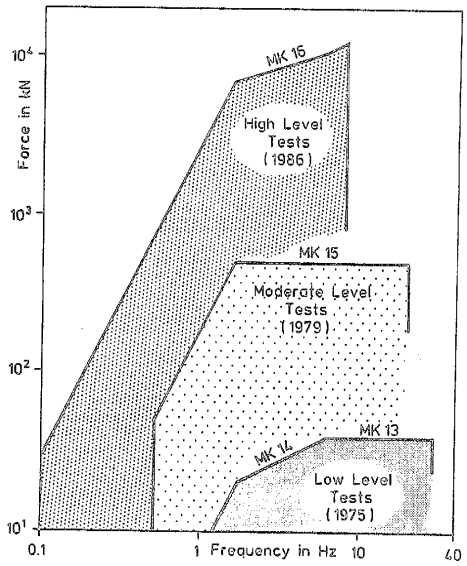

Fig.5: Shaker Force and Frequency Ranges

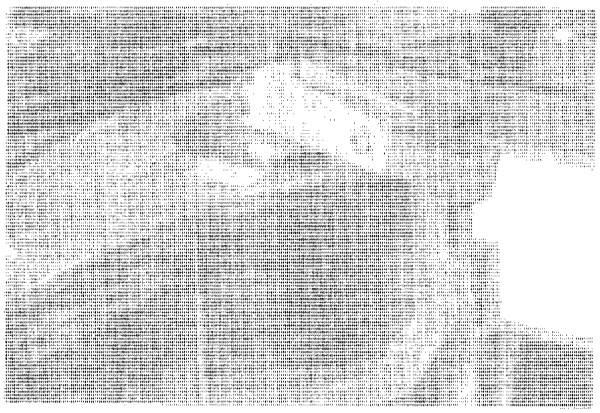

Fig.6: MK 14 Eccentric Mass Shaker (1975)

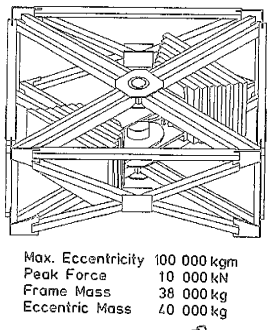

Max. Eccentricity 100 000 kgm
Peak Force 10 000 kN
Frame Mass 38 000 kg
Eccentric Mass 40 000 kg

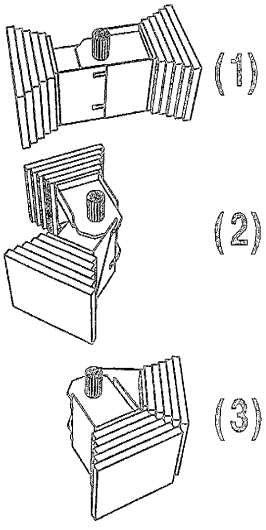

Fig.7: MK 16 Coast-Down Eccentric Mass Shaker (1986)

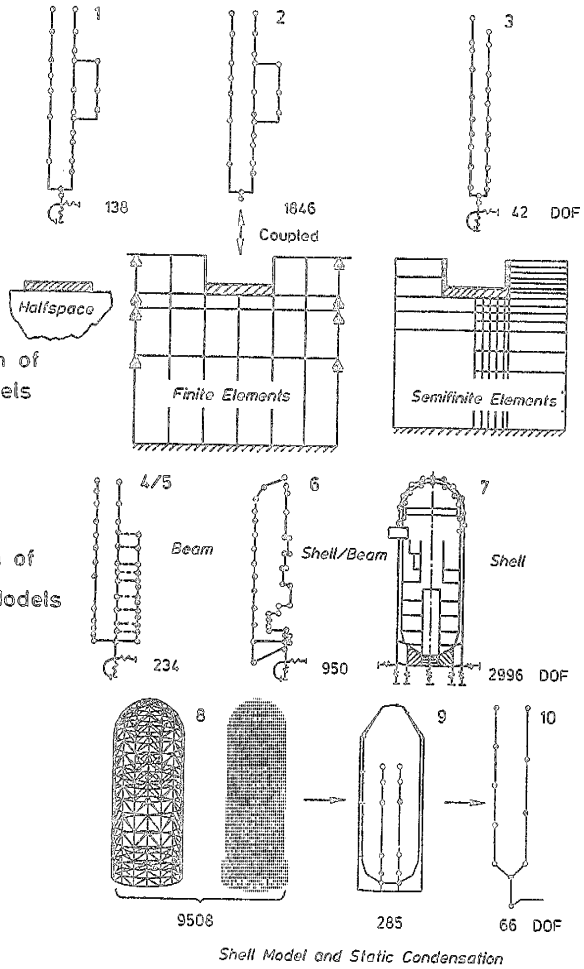

Fig.8: Reactor Building and Soil Models

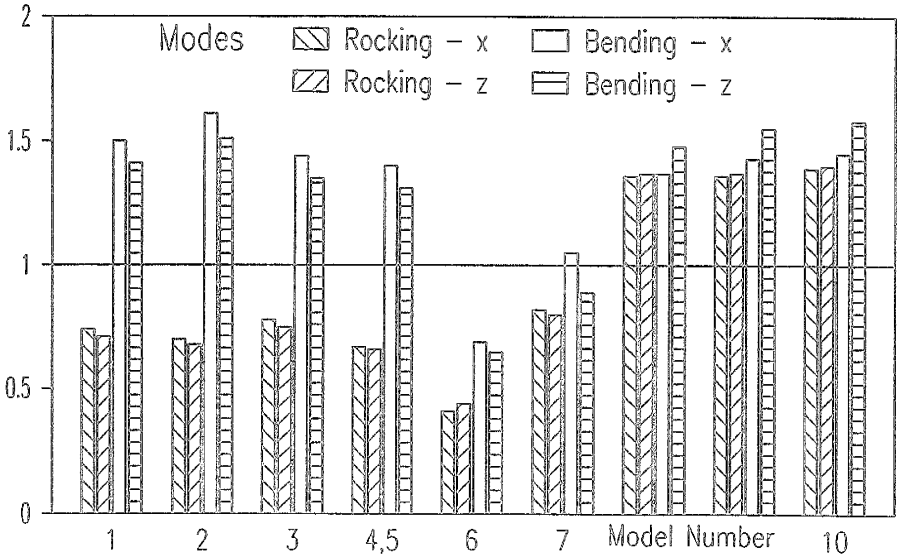

Fig.9: Ratio of Calculated to Measured Natural Frequencies

Structural Component	Design Limit Load	Best Estimate Limit Load	Observations During Tests
Internal Concrete Structure	1.37	0.67	Minor Cracks in Stair Case (not critical)
Basement			
Intermediate Floor -8 m	10.0	3.00	Large Cracks Through Floor (not critical)
Foundation Slab	3.00	1.75	No Cracks Detected in Base Slab
External Concrete Structure			
Basement Region	5.26	3.30	No Cracks Detected in Outer Wall
Cylindrical Shell	1.52	1.02	Test Load Limiting Component
Sliding of Steel Containment in Egg - Cup	1.67	1.10	No Sliding Measured
Basemat - Uplift	0.96	0.84	No Uplift Observed
Soil Failure	1.61	0.94	Foundation Settlement 3 to 11 mm

Fig.10: Achieved Load in Multiples of Calculated Ultimate Loads of Reactor Building Structures

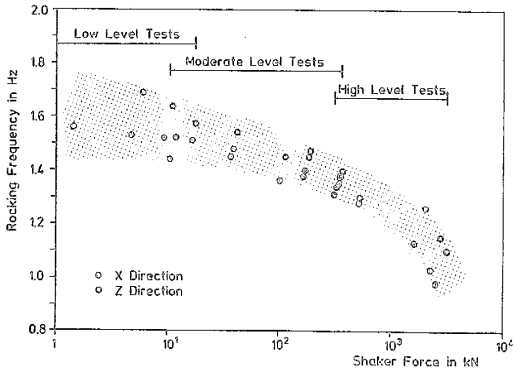

Fig.11: HDR Rocking Frequency versus Shaker Force

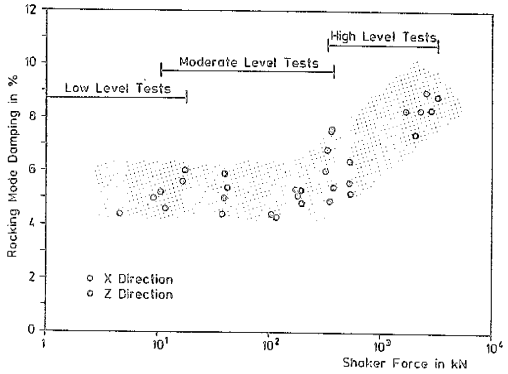

Fig.12: Rocking Mode Damping versus Shaker Force

Fig.13: Reactor Pressure Vessel Vibration Behavior

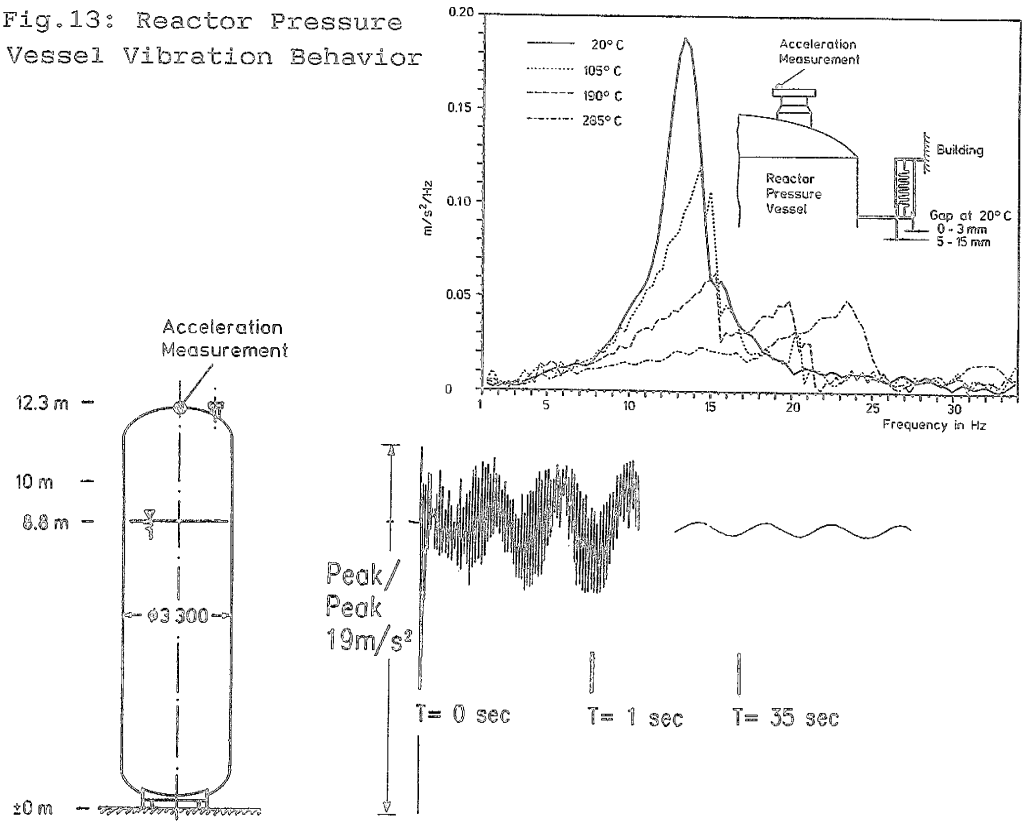

Fig.14: Flood Water Storage Tank Vibration Behavior

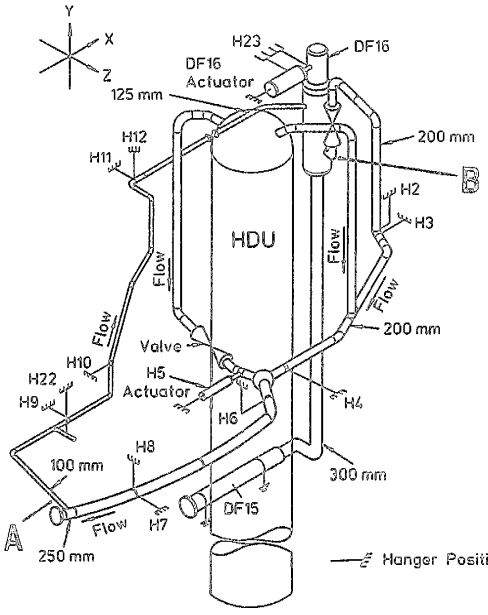

Fig.15: Test Loop VKL

Hanger No.	Hanger Configuration NRC 3	EPRI/SS 5	EPRI/EA 4	CEGB 6	KWU 2	HDR 1
4						
23						
9						
10						
11						
8						
7						
12						
3						
22						
6						
2						

Hanger Positions
Strut
Energy Absorber
Snubber
Seismic Stop

Fig.16: VKL Support Configurations

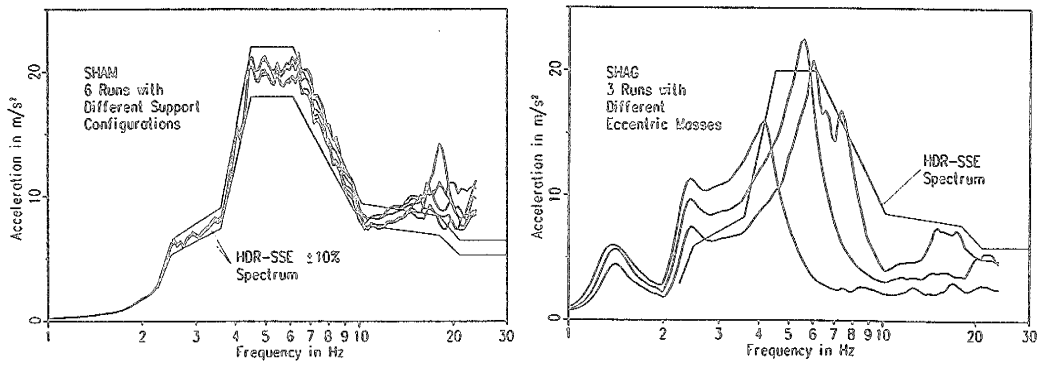

Fig.17: Response Spectra (D=4%) of VKL Input Acceleration during SHAG and SHAM Tests

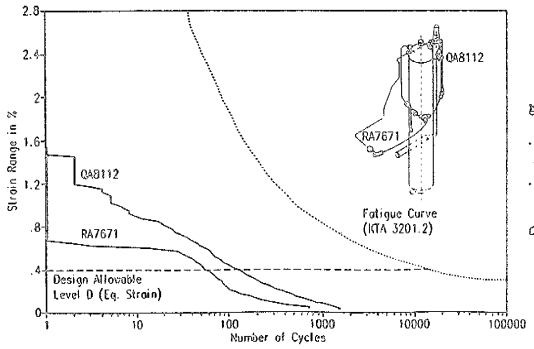

Fig.18: Strain Cycles Accumulated during SHAM Tests

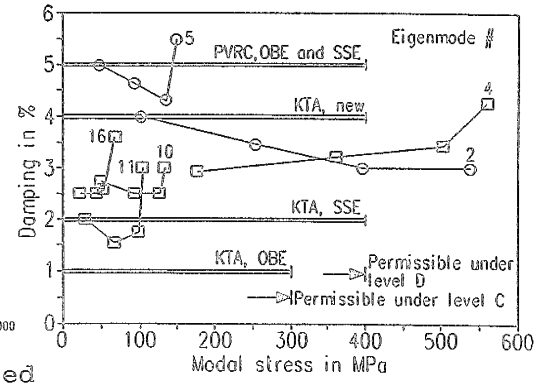

Fig.19: VKL Modal Damping Versus Modal Stress

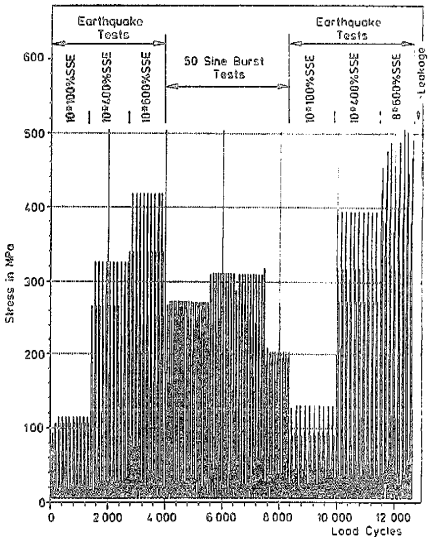

Fig.20: Bending Stress Time History at Predamaged Pipe Cross Section

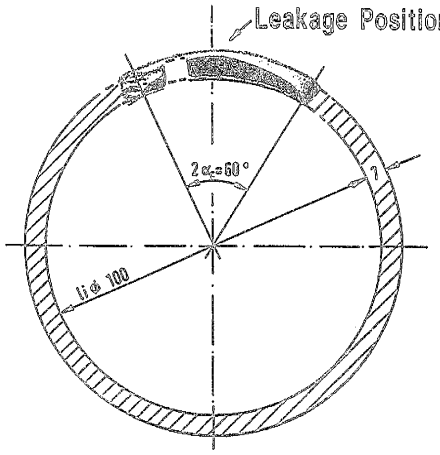

Fig.21: Crack Shape of Failed Pipe Cross Section